IEEE Access
Multidisciplinary | Rapid Review | Open Access Journal

Received 10 February 2024, accepted 4 March 2024, date of publication 12 March 2024, date of current version 21 March 2024.

Digital Object Identifier 10.1109/ACCESS.2024.3375349

RESEARCH ARTICLE

Experimental Implementation of Hydraulic Turbine Dynamics and a Fractional Order Speed Governor Controller on a Small-Scale Power System

CLAUDIA SABRINA MONTEIRO DA SILVA[1,3,4], NEI JUNIOR FARIAS DA SILVA[1,4], FLORINDO A. DE C. AYRES JÚNIOR[1,3,4], RENAN LANDAU PAIVA DE MEDEIROS[1,3,4], LUIZ EDUARDO SALES E SILVA[1,3,4], AND VICENTE FERREIRA DE LUCENA JR.[2,3,4], (Senior Member, IEEE)

[1]Department of Electricity, Federal University of Amazonas—UFAM, Manaus 69080-900, Brazil
[2]Department of Electronic, Telecommunication and Computation, Federal University of Amazonas—UFAM, Manaus 69080-900, Brazil
[3]Center of Research and Development in Technology, Electronic and Information—CETELI, UFAM, Manaus 69080-900, Brazil
[4]Graduate Program in Electrical Engineering—PPGEE, UFAM, Manaus 69080-900, Brazil

Corresponding author: Renan Landau Paiva De Medeiros (renanlandau@ufam.edu.br)

This research, carried out within the scope of the Samsung-UFAM Project for Education and Research (SUPER), according to Article 39 of Decree n°10.521/2020, was funded by Samsung Electronics of Amazonia Ltda., under the terms of Federal Law n°8.387/1991 through agreement 001/2020, signed with Federal University of Amazonas (UFAM) and Federal Institute of Amazonas (IFAM) Teaching, Research, Extension and Internalization Support Foundation (FAEPI), Brazil. The authors thank the scholarship and financial support in part from the Amazonas State Research Support Foundation (FAPEAM), Foundation Coordination for the Improvement of Higher Education Personnel (CAPES), National Council for Scientific and Technological Development (CNPq) and UFAM. Thanks to the College of Technology of UFAM (FT/UFAM) Control Systems (LC) and Electrical Machines Laboratory (LME) at UFAM and the e-Controls Research Group.

ABSTRACT In this paper, the practical application of automatic control techniques is performed to enhance the performance of the isochronous speed regulator of hydraulic turbines, thus making the electrical power system more efficient. To achieve this, the dynamic model of the 2kVA small-scale power system is employed for controller tuning. This system encompasses a synchronous generator and a coupled DC motor, with the hydraulic turbine dynamics incorporated into a microcontroller that replicates the behavior of larger power plants. For this purpose, a fractional-order PID controller (FOPID) is developed, given that this controller offers two additional degrees of freedom for design purposes. Therefore, in the design of the FOPID controller, a methodology based on analytical values of gain and phase margin is used. Additionally, a classical PID controller is tuned using the pole placement method to match the performance of both controllers. The aim of the study is to assess the effectiveness of the proposed methodology through comprehensive computational simulations and practical experimental tests, considering variations in the reference value and load, and qualitative analysis through temporal and quantitative analysis, using performance indices. The results demonstrate that the proposed methodology outperforms other approaches and confirms its effectiveness and flexibility. Thus, this article significantly contributes to the field of power generation system control, highlighting the importance of experimental validation to ensure performance in real-world scenarios.

INDEX TERMS Fractional order controller, hydraulic turbine dynamics, isochronous speed governor, small-scale power system.

NOMENCLATURE

λ	Non-integer order integrator coefficient.
μ	Non-integer order derivative coefficient.
k_p	Proportional gain.
k_I	Integral gain.
k_D	Derivative gain.
ω_{gc}	Gain crossover frequency.
ω_{pc}	Phase crossover frequency.

The associate editor coordinating the review of this manuscript and approving it for publication was Nasim Ullah.

$\Delta\omega_{ref}$	Speed setpoint variation.
ΔT_{load}	Mechanical load insertion into the system.
ω	Angular speed.
u	Speed regulator control signal.
$p.u.$	Per unit.
DC	Direct current.
SG	Speed Governor.
FOPID	Fractional Order PID.
PFOPID	Practical FOPID.
SFOPID	Simulated FOPID.
PP	Pole Placement.
PPP	Practical PP.
SPP	Simulated PP.
ISE	Integral Square Error.
IAE	Integral Absolute Error.
ITAE	Integral Time Absolute Error.
ITSE	Integral Time Square Error.
ISC	Integral Square Control Efforts.

I. INTRODUCTION

The intensive economic and social development causes electrical energy demand growth, requiring new-generation plants and the capacity expansion of existing ones. However, in complex and sophisticated electric power systems (EPS), dynamic problems on machines arise, such as electric frequency regulation, voltage regulation, and energy supply.

Currently, the hydroelectric plant stands out among large electric power generation systems due to the pioneering spirit of applying sophisticated control methodologies to ensure the system's reliability, performance, and security. This unit comprises a water tunnel, penstock, surge tank, hydraulic turbine, speed governor (SG), generator, and electrical network [1]. The hydraulic turbine converts kinetic energy into mechanical energy [2] and, when coupled to a synchronous machine, transforms mechanical energy into electrical energy [3].

Constant electrical frequency is critical for synchronous machines to deliver power safely and effectively to a load or electrical system [4]. Furthermore, it becomes one of the requirements of correct synchronism and operation loads with reactive characteristics. To keep this frequency constant, several methods can be used, such as speed governors [1], electronic power circuits for generation sources with variable speed [5], or specifically, on interconnected systems, power system stabilizers to maintain the stability of the system when electrical power fluctuations occur at low frequencies [6].

The speed governor aims to keep the electric frequency within the tolerance range. For that, the power produced by unit generating must be near that developed by the primary machine [2]. In this operation, the regulator must use a speed sensor to detect acceleration or deceleration. Then, the regulator will make the system decrease or increase mechanical power delivered to the synchronous machine rotor [4].

Consequently, various hydraulic turbine models and their speed governors are employed in research related to energy systems of multiple types. These models encompass the primary driving machinery, including water supply conduits and machine speed controls. The need for nonlinear models is recognized in scenarios where significant changes in speed and power occur, as in studies of islanding, load shedding, and system restoration, providing a fundamental understanding of the physics of hydraulic turbines and their respective controls. This acknowledges that, in practice, developing code for a specific model is a common task as long as the physical principles of the system are well-defined [7].

The controller monitors and adjusts the turbine's speed to ensure compliance with the desired operational requirements. Various controller design approaches are employed in implementing speed regulators to enhance system efficiency. Currently, PID (Proportional Integral Derivative) controllers are widely used in the operation of hydroelectric turbines, despite their simplicity. However, they have limitations in their ability to deal with disturbances, uncertainties, and error integration. In this context, in [8], a model predictive control (MPC) based controller was developed and applied to a laboratory hydroelectric plant in a simulation environment. The results revealed that MPC outperforms the classic PID controller, highlighting its potential for practical implementation. However, relevant research presented a controller with variable gain according to the hydro generation system gate opening to decrease the effects of non-linearity of the plant and improve the dynamic performance [9], [10].

In [11], a technique known as chaotic butterfly optimization (CBOA) was utilized to fine-tune cascade PI-TID (Proportional Integral tilt-integral-derivative) controllers, aiming to meet gain constraints within the context of load frequency control of dual area hybrid microgrid (DHM). Furthermore, the application of CBOA was employed to optimize the PI-TID controllers. In [12], an identification methodology obtains a model of the machine connected on an infinite bus for use on speed governor design for a generating unit connected to the electric power system. The authors in [13] used a controller with fuzzy sets to update the Proportional Integral Derivative (PID) controller parameters online for electrical frequency regulation. In [14], a nonlinear sliding mode controller was applied with parameters updated using measurements performed during the controller operation. This dispenses with the need for the mathematical model of the plant applied to the frequency regulation of microgrids present in ships.

In [15], a strategy of cooperative control of wind power generators and plug-in electric hybrid vehicles to primary frequency regulation of a microgrid. This study employed a small signal analysis to investigate which frequency regulation method, droop or virtual inertia, is more suitable for such cooperation. Furthermore, centralized and distributed control structures are evaluated as two possible coordination methods to ensure that the wing generator and plug-in electric hybrid vehicle constraints are not violated. Finally,

to assess the performance of the proposed methodology, several simulations were carried out in the time domain using a typical microgrid system.

If the frequency transmitted exceeds standard limits, recovery of the load-generation balance is needed. Although the controller designed by conventional methods has been widely applied to the hydro turbine speed governor system, a much more effective and reliable control law is required for a hydroelectric plant [1]. To make these systems more reliable, the mathematical concept of fractional order calculation began to be used in control systems and other areas of engineering. Reference [16] discusses the fractional order design method for typical second-order installations.

Recent practical works using fractional control are seen in some articles, as in [17], where a new methodology for polynomial pole placement using commensurable fractional transfer functions applied in the voltage regulation of a Buck topology DC/DC converter is studied, [18] the use of optimization algorithms to obtain fractional compression ignition models in standard rail systems are investigated, and in [19] fractional observers for harmonic disturbances for a three-phase LCL-type inverter system, aiming to effectively eliminate all multi-frequency disturbances, thus aiming at a significant increase in the quality of the electric current output. In [20], the design of a robust controller with fractional characteristics for a three-phase autonomous voltage source converter was presented. In [21] shows the superiority of fractional controllers over their conventional equivalents for applications in Networked Control Systems and process control. In [22], a FOPID controller based on advanced fuzzy logic is used to deal with changes in the dynamics of a nuclear reactor with an operational power level.

In [23], the fractional order fuzzy-pid controller is used to regulate the frequency of a tidal and diesel power plant hybrid system. In [24], is investigated the applicability of fractional order (FO) intelligent control for hybrid power systems or distributed energy generation and the controller parameters are tuned using robust optimization techniques employing different variants of particle swarm optimization (PSO) and were compared with the corresponding optimal solutions using simulational results. In [1] depicts a Fractional Order Proportional Integral Derivative (FOPID) implemented with active-disturbance-rejection-control (ADRC) to perform online parameters controller update.

The study conducted in [25] assesses the stability of four controllers, including PID, PID with second-order derivative, FOPID, and FOPID with second-order derivative, in a hydraulic turbine system with fractional-order parameters and time delay. After analyzing the impact of controller parameters in simulated experiments, the results indicate that the FOPID with second-order derivative controller outperforms the other controllers in terms of stability. However, to enhance the hydraulic turbine's response to load disturbances, [26] investigates the application of a FOPID controller to the hydraulic turbine governor based on a nonlinear model. The optimal parameters are found using the particle swarm optimization (PSO) algorithm. In [27], the design of a FOPID controller for a hydraulic turbine regulating system is accomplished through the chaotic non-dominated sorting genetic algorithm II (NSGAII), used as an optimizer to discover the set of optimal solutions for the FOPID. This enables designers to select solutions based on the priority of objective functions. The results, including simulations and experiments, confirm the superior performance of fractional-order controllers over integer-order controllers.

To the best of the authors' knowledge, the literature presents a lack due to few works performing an experimental investigation of the fractional order controllers applied in power system testbeds. In [28], a practical application of fractional-order controllers in a hydrogeneration system is investigated, where a fractional order Power System Stabilizer (PSS) was designed to damp the electromechanical oscillation mode that has low damped and may cause undesired oscillations and may evolve to instability of the system. The practical tests were carried out in six operations points, presenting an enhancement in the performance behavior of the behavior of the 10 kVA small-scale.

As mentioned throughout this context, various contemporary controllers employing optimization algorithms have been applied to electric turbine speed regulation. However, the FOPID controller has garnered significant attention due to its inherent flexibility in design compared to the conventional PID control structure. Nevertheless, the practical implementation of the FOPID controller has seen limited utilization in power generation systems. Therefore, the relevance of this study lies in its experimental approach, providing valuable insights into how the FOPID controller can be effectively implemented in a real-world environment. This is a significant contribution since much of the available literature often relies on theoretical simulations, while experimental validation is essential to ensure the controller's effectiveness in practical scenarios.

Thus, in this work, an experimental application and design of a fractional order PID methodology as an isochronous speed governor of the small-scale power system are investigated to regulate the electrical frequency of the electrical power system. Therefore, a linearized mathematical model of the 2 kVA reduced-scale power generation system is used to design two controllers, such as a conventional PID controller based on the integer-order pole placement technique as presented in [29] and the proposed methodology by using the FOPID control structure. After that, the system's dynamic behavior with both controllers' insertions is compared. Then, experimental tests on a small-scale system testbed are performed. Controller laws and hydraulic turbine dynamics are implemented in an embedded system using *Arduíno Due* microcontroller.

The main contributions of this study can be summarized as follows:

- The practical application of a methodology for designing a fractional-order controller using desired gain and phase margins, adapted from [30], to improve system performance.
- Several experimental tests on a small-scale power system were made, which included a synchronous machine and a coupled DC motor that emulates the dynamics of a hydro-generation system embedded in the microcontroller.
- The proposed work shows that the FOPID methodology enhances system operation by increasing the degree of freedom and comparing the fractional controller with a classical pole placement method to illustrate the superior performance of the proposed methodology over other approaches.

The remainder of this paper is organized as follows: Section II shows the hydraulic generation system focusing on main components and dynamic models. The hydro generation parameters system and the methodology applied for FOPID speed governor design are shown in section III. Section IV highlights results obtained by the FOPID controller compared to an integer-order controller obtained by the pole placement method through the speed response and control effort due to step speed command variation. Finally, conclusions are drawn in section V.

II. HYDROGENERATION UNIT

The hydroelectric power plant generation system transforms kinetic energy from water displacement into mechanical energy through a hydraulic turbine, coupled to the synchronous generator, to convert mechanical energy into electrical energy [2].

Hydraulic turbines can be classified into action or reaction turbines, which are applied according to fall height and water flow. The regulators can be isochronous (without droop) or with permanent droop (with speed drop). The isochronous speed governors theoretically maintain the turbine speed constant and work satisfactorily when a generator is feeding an isolated load or when only one generator in a multi-generator system is needed to load variations respond. The regulators with droop have a speed drop characteristic, which is necessary for a stable load division between two or more generating units operating in parallel. In this work, the isochronous SG characteristics are used [2].

A. HYDRAULIC TURBINE MODELING

The dynamics of the hydraulic turbine are described by the most straightforward configuration, with water and the forced conduit walls considered incompressible.

Where $\overline{G}$ is the gate ideal opening; A_t is the hydraulic turbine gain; $\overline{g}$ is the actual opening of the gate; $\overline{H}$ is the lake height; $\overline{U}$ is the water speed in the turbine; $\overline{U_{nl}}$ is water speed with the turbine running without load; $\overline{H_o}$ is the initial hydraulic drop; $\overline{P_m}$ is the mechanical power developed by the turbine; $\overline{\omega}$ is the speed of the turbine-generator set; $\overline{T_m}$ is the mechanical torque developed by the turbine; T_ω is the starting time of the water; $\overline{P_r}$ is the change of base; [2] given by (1).

$$\bar{P}_r = \frac{\bar{P}_t}{\bar{P}_b} \tag{1}$$

therefore $\overline{P_t}$ is the nominal power of the turbine; $\overline{P_b}$ is the power system base.

The most straightforward hydraulic turbine configuration has been exhibited, with water and the forced conduit walls considered incompressible. This model is the most appropriate for studying large signals in the time domain.

The hydraulic turbine transfer function is obtained from linearization based on an expansion of Taylor's series of the mathematical model around operation point $\overline{U_o}$, $\overline{G_o}$, $\overline{H_o}$ and $\overline{P_{mo}}$, considering ideal gate opening and rated turbine speed. The linearized equation, shown in (2), is used in small signal stability studies and controller design [2].

$$G_1(s) = \frac{\bar{P}_m(s)}{\bar{G}(s)} = \frac{1 - T_\omega s}{1 + \frac{1}{2}T_\omega s} \tag{2}$$

B. SERVO POSITIONER MODELING

The servo positioner is an electro-hydraulic system that detaches blades from the hydraulic turbine gate. This movement is carried out using command signals from the gate opening straight from the control laws of the speed regulator. After hydraulic drive system modeling, the state space model presented in (3) to (5) is obtained.

$$\begin{bmatrix} \dot{x}_1 \\ \dot{x}_2 \end{bmatrix} = \begin{bmatrix} 0 & \frac{1}{t_g} \\ -\frac{1}{t_p} & -\frac{1}{t_p} \end{bmatrix} \begin{bmatrix} x_1 \\ x_2 \end{bmatrix} + \begin{bmatrix} 0 \\ \frac{1}{t_p} \end{bmatrix} u \tag{3}$$

$$g_{min} \leq x_1 \leq g_{max} \tag{4}$$

$$y = \begin{bmatrix} 1 & 0 \end{bmatrix} \begin{bmatrix} x_1 \\ x_2 \end{bmatrix} \tag{5}$$

where, u is the speed regulator control signal; t_p is the resulting time constant for the pilot servo motor (in seconds), pilot valve, and proportional controller K_1; t_g is the resulting time constant for the main servo motor (in seconds), gate valve and proportional controller K_2; g_{min} is the servomotor minimum displacement and g_{max} is the servo motor maximum displacement.

Considering, $t_p \ll t_g$, the mathematical model of the servo positioner is simplified for the transfer function given in (6) [31].

$$G_2(s) = \frac{X_1(s)}{U(s)} = \frac{1}{t_g s + 1} \tag{6}$$

C. INERTIA CONSTANT AND VISCOUS FRICTION OF TURBINE GENERATOR COUPLING

In the emulation process of the small-scale generation system, a direct current motor converts electrical energy into mechanical energy. The engine's electrical dynamics are neglected and changed by mechanical dynamics, such as inertia constant and viscous friction of the generator coupling

FIGURE 1. Power generation system of small scale of 2 kVA.

TABLE 1. Hydraulic turbine, servo positioner and DC motor parameters.

Parameters		Unit	Value
Minimum opening of the gate	g_{min}	s	0.06
Maximum opening of the gate	g_{max}	s	0.96
Turbine gain	A_t	-	1.11
Nominal hydraulic lake drop	H_o	p.u.	1.0
Time of water start	T_ω	s	1.41
No-load water speed	U_{nl}	p.u.	0.068
Base change	P_r	-	1.0
Pilot valve time constant	t_p	s	0.016
Distribution valve time constant	t_g	s	2.8
Moment of motor inertia	H	s	0.68
Viscous friction	$\bar{B}$	p.u.	0.11

with the turbine. The DC motor emulation model transfer function is given by (7) [2].

$$G_3(s) = \frac{\bar{\omega}}{\bar{P}_t} = \frac{1}{2Hs + \bar{B}} \tag{7}$$

where, H is the inertia moment of motor and $\bar{B}$ is the viscous friction in $p.u.$ (per unit).

III. TUNING PARAMETERS OF SPEED GOVERNOR CONTROLLERS

A. SYSTEM TRANSFER FUNCTION OF SMALL SCALE POWER GENERATION

For the controllers' development, simulation, and tests, a small-scale power generation system was used, consisting of a 2kVA generator set, as presented in Fig. 1. This system has an independent excitation DC motor that drives the synchronous pole machine.

The system parameters were obtained through tests carried out in a laboratory environment, some of which are presented in Table 1.

In the SG controllers setup gains, the linearization performed previously originated a transfer function representing a small-scale hydro generation system. The cascaded transfer function is shown in (8) is clustering the physical rotational dynamics of the synchronous machine, hydraulic turbines transfer function, and servo positioner transfer function, where the system output variable is the angular speed in the machine rotor.

$$G_s(s) = \left(\frac{1 - T_\omega s}{1 + \frac{1}{2}T_\omega s}\right)\left(\frac{1}{t_g s + 1}\right)\left(\frac{1}{2Hs + \bar{B}}\right) \tag{8}$$

Applying T_ω, t_g, H and $\bar{B}$ values presented in Tables 1 in (8) is obtained the transfer function (9), which shows this plant has a zero in right semi plane, in other words, it is a non-minimum phase system.

$$G_s(s) = \frac{-0.5252\, s + 0.3725}{s^3 + 1.8565s^2 + 0.6502s + 0.0410} \tag{9}$$

In a laboratory test-bed system, the DC motor coupled to the synchronous generator, together with a microcontroller, performs the mechanical dynamics emulation of the micro-machine. The microcontroller has the function of emulating the dynamics of the servo-positioner and the hydraulic turbine, controlling the power of the DC motor, and making the speed regulation of the system.

Fig. 2 presented the operation of the emulator presented in this paper. The emulation system comprises three main components: the Arduino Due, the buck circuit, and the DC motor. The Arduino is responsible for developing the dynamic of the speed controller projected in this paper, electrical turbine, and power controller so that the mechanical power of the engine is equal to that of the emulated hydraulic turbine. The buck triggers the DC motor that has mechanical dynamic similarity to a hydraulic turbine operating isolated.

The speed governor utilizes the speed developed for the DC motor emulating the turbine for realized a regulation of the speed of the turbine, and the controller of power uses armor current and the speed for the controller the mechanical power of DC motor employing a buck converter to variate the voltage at the armature terminal.

B. FOPID CONTROLLER TUNE

The FOPID controller is a type of PID controller with an extra degree of freedom in its derivative and integral parts due to the application of fractional calculus application [1]. A relationship with the classic PID controller is shown in Fig. 3, with the FOPID controller extending into the shaded area and the more prominent first quadrant of the region [26]. The integro-differential equation defining a control action of a FOPID is expressed in (10) [30].

$$C(s) = k_p + \frac{k_I}{s^\lambda} + k_D s^\mu,\ (\lambda > 0,\ \mu > 0) \tag{10}$$

where, s is Laplace's operator, λ is a non-integer order integrator coefficient, and μ is the derivative coefficient [1]. The additional parameters λ and μ can admit any real number value [32].

One of the most significant FOPID controller advantages is the better control of dynamical systems and less sensitive parametric variations of a controlled system [32]. Hence,

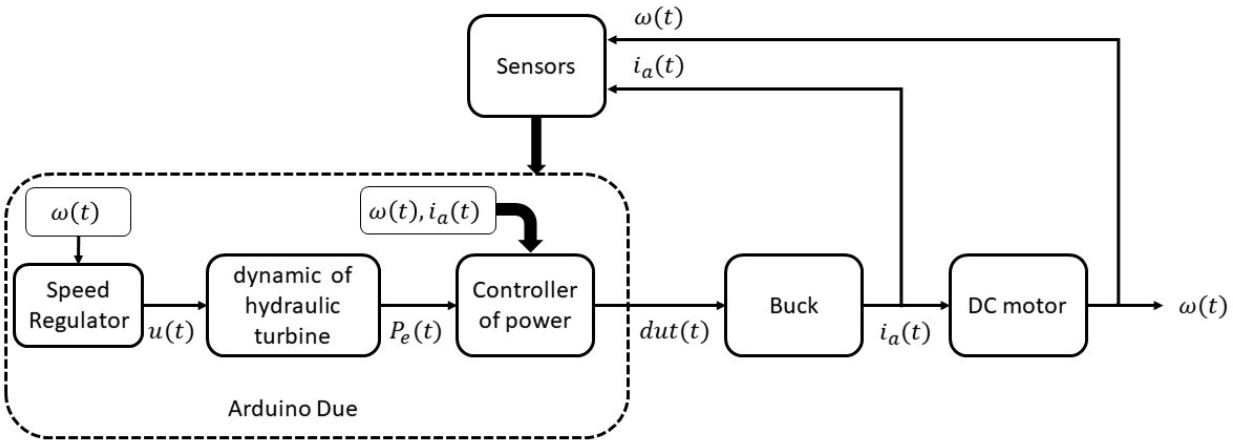

FIGURE 2. Emulation system scheme.

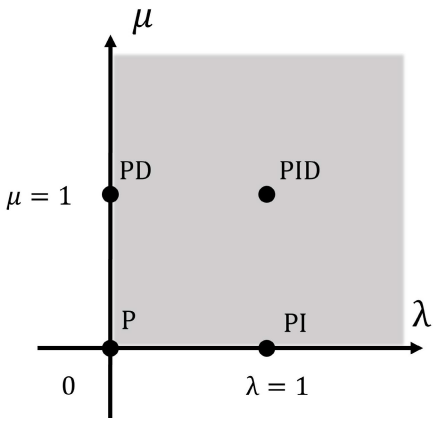

FIGURE 3. The relationship between the FOPID controller and the conventional PID controller.

an improvement in dynamic behavior is expected. This occurs because the FOPID controller has five adjusting parameters, two more when compared to classical PID controllers. These extra degrees turn a fractional control system better adjusted on dynamical properties [33].

Including two additional degrees (λ and μ) of freedom in fractional-order PID controllers is based on the inherent flexibility of these controllers. This flexibility represents a significant departure from the conventional approach used in integer-order systems, which is constrained to the left half of the complex plane. The evidence of the impact of fractional order in various regions of the system, subject to adjustments, whether compressing or expanding these regions based on the value of the fractional parameter, becomes evident when these control structures are applied. This characteristic is a direct consequence of the theoretical framework that underpins this class of controllers.

Comparing FOPID and conventional PID, the adjustable parameters of non-integer order, derivative, and integrator grant flexibility to obtain the desired dynamical control performance [1]. Currently, the fractional-order interval (λ and μ) varies from 0 to 2. However, in most previous research works, variation happens between 0 to 1 [34] due to the stability region of fractional-order systems.

Currently, several methods for tuning FOPID controllers [30] are divided into analytical, numerical, and rule-based. In many cases, the adjustment process automation is possible with appropriate tests to find the plant parameters for the adjustment [35]. The analytical method based on gain and phase margin values obtains parameter values of the FOPID controller, k_p, k_I, k_D, λ and μ from target gain and phase margin values for Single Input Single Output (SISO) closed-loop system [35].

$$k_p + \left(\frac{k_I}{\omega_{gc}{}^{\lambda}} \cos\left(\frac{\lambda\pi}{2}\right)\right) + k_D\omega_{gc}{}^{\mu} \cos\left(\frac{\mu\pi}{2}\right) = \frac{\cos\left(-\pi + \varphi_m - \angle(G(j\omega_{gc}))\right)}{|G(j\omega_{gc})|} \tag{11}$$

$$\left(-\frac{k_I}{\omega_{gc}{}^{\lambda}} \sin\left(\frac{\lambda\pi}{2}\right)\right) + k_D\omega_{gc}{}^{\mu} \sin\left(\frac{\mu\pi}{2}\right) = \frac{\sin\left(-\pi + \varphi_m - \angle(G(j\omega_{gc}))\right)}{|G(j\omega_{gc})|} \tag{12}$$

$$k_p + \left(\frac{k_I}{\omega_{pc}{}^{\lambda}} \cos\left(\frac{\lambda\pi}{2}\right)\right) + k_D\omega_{pc}{}^{\mu} \cos\left(\frac{\mu\pi}{2}\right) = \frac{\cos\left(\pi - \angle(G(j\omega_{pc}))\right)}{g_m|G(j\omega_{pc})|} \tag{13}$$

$$\left(-\frac{k_I}{\omega_{pc}{}^{\lambda}} \sin\left(\frac{\lambda\pi}{2}\right)\right) + k_D\omega_{pc}{}^{\mu} \sin\left(\frac{\mu\pi}{2}\right) = \frac{\sin\left(\pi - \angle(G(j\omega_{pc}))\right)}{g_m|G(j\omega_{pc})|} \tag{14}$$

To implement the FOPID controller, the classical Oustaloup approximation was applied. The Oustaloup approximation guarantees an integer equivalent with N real stable poles and zeros restrained in frequency bandwidth, high and low $[\omega_l, \omega_h]$ [35].

TABLE 2. Controller parameters.

Parameters		Unit	Value
Settling time	t_s	s	45
Maximum overshoot	M_{ss}	-	0.1
Error	e	%	5
Damping factor	ζ	-	0.5912
Natural frequency	ω_n	rad/s	0.1126
Gain margin	gm	dB	6
Phase margin	φ_m	°	65
Gain crossover frequency	ω_{gc}	rad/s	0.1126
Phase crossover frequency	ω_{pc}	rad/s	0.5631

Therefore, the FOPID controller uses the same parameter design presented in Table 5. Remember that the gain and phase margin values and the gain and phase crossing frequency were chosen through the heuristic method, aiming at a stable closed-loop system. However, this work uses a particular case, where $\lambda = 1$ and the values of k_p, k_I, k_D and μ are obtained through the analytical method of gain margin and phase margin method that uses the four non-linear equations ((11) to (14)), developed in [35].

Hence, after computing the set of four non-linear equations, applying the Matlab command "solve" and using the desired performance constraints given by 5, using the numerical method tolerance less than 10^{-8}, and considering $\lambda = 1.0$, the FOPID controller parameters were obtained as $k_p = 0.1651$, $k_I = 0.0129$, $k_D = 0.1678$, and $\mu = 0.8220$. After defining the parameters, the Oustaloup method was applied for a fourth-order approximation, using $\omega_l = 0.0398$ (rad/s), $\omega_h = 0.3185$ (rad/s). The equivalent integer order FOPID controller transfer function is given by (15), as shown at the bottom of the page.

Fig. 4 shows the Bode diagram of the FOPID controller for frequencies between 10^{-2} and 10^{2} (rad/s), where the blue line represents the FOPID controller without approximation and its integer order equivalent for the chosen bandwidth of approximation by the Oustaloup method (dashed black line), where is shown that the approximation fits well the desired bandwidth choose in the project.

To compare the behavior of the investigated FOPID controller, a controller was tuned by the classic pole placement method [29], using the Diophantine equation and the same design characteristics presented in 5. The parameters of the classical controller were calculated through a pole placement technique employed to adjust the controller so that, in a stable closed-loop system, it meets the desired specifications, such as maximum overshoot, settling time, and natural frequency, among other performance metrics.

TABLE 3. Digital controllers parameters.

Parameters	Classic PP	FOPID
r_0	-0.3465	0.2305
r_1	1.033	-1.138
r_2	-1.025	2.246
r_3	0.3392	-2.217
r_4	-	1.094
r_5	-0.3465-	-0.216
s_1	-2.939	-4.935
s_2	2.882	9.742
s_3	-0.9431	-9.615
s_4	-	4.744
s_5	-	-0.9365

Thus, we shifted the system's poles to a new position that satisfied these performance criteria.

The obtained controllers were discretized to apply the controllers in the emulated embedded system. The Tustin method was applied to implement the practical controllers with a sampling time of $T = 0.1\ s$ using the digital control structure presented in (16). Table 3 gives the parameters of both digital controllers investigated (Pole Placement and FOPID) [36].

$$C(z) = \frac{\sum_0^{n=\infty} r_n z^{-n}}{1 + \sum_1^{m=\infty} s_m z^{-m}} \tag{16}$$

The controller was designed for the frequency bandwidth between $\omega_l = 0.0398\ rad/s$ and $\omega_h = 0.3185\ rad/s$ and was observed that for the frequencies included in the bandwidth approximation and for frequencies below the bandwidth, the values were very close, both in magnitude and in phase, confirming the gain and phase margin selected for this project.

IV. RESULTS

This section presents and discusses the simulational and practical results obtained by the small-scale testbed system of 2 *kVA* developed.

A. BRIEF DESCRIPTION OF THE DEVELOPED TESTS

Three tests are performed to evaluate the performance and stability of each control methodology, focusing on developing a quantitative and qualitative analysis of each methodology. These tests are briefly described as follows:

The first test aims to evaluate the system's behavior when a setpoint speed variation is performed. Initially, the started system waits for the turbine to accommodate at 1.0 p.u. of rotation speed reference. Then, the reference is decreased in steps of 0.05 *p.u.* and 0.1 *p.u.* of speed and, in the sequence, incremented in steps of the same size until reaching the speed of 1.0 *p.u.*

$$C_2(s) = \frac{0.2306\ s^5 + 0.1493\ s^4 + 0.0365\ s^3 + 4.216.10^{-3}s^2 + 0.2321.10^{-3}s + 4.895.10^{-6}}{s^5 + 0.6564\ s^4 + 0.1450\ s^3 + 0.0128\ s^2 + 0.378.10^{-3}s} \tag{15}$$

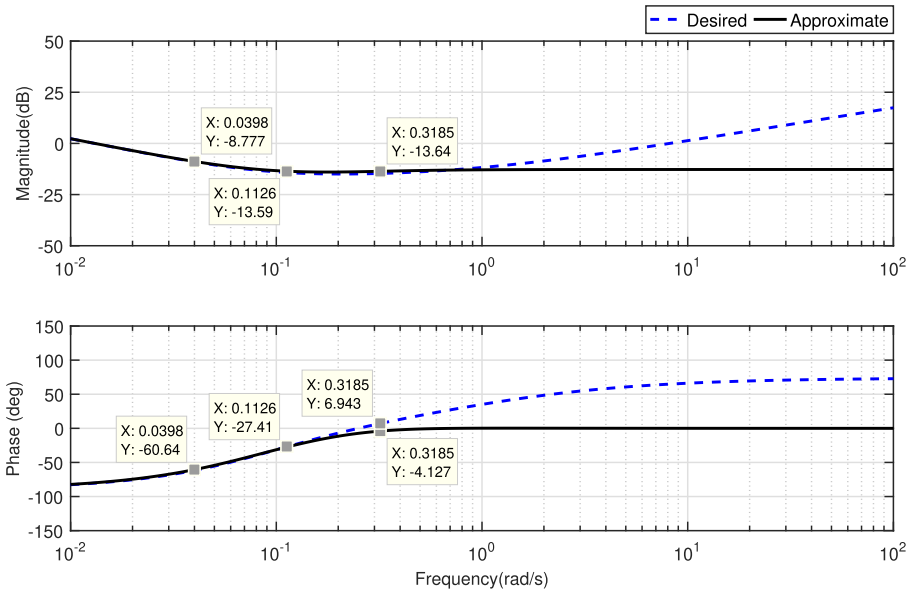

FIGURE 4. Bode diagram of FOPID controller.

The second test evaluates the system's behavior when inserting the electromechanical load. Initially, the system is started, and the turbine can settle at 1.0 per unit (*p.u.*) of rotation speed reference. Next, four loads of 0.005 *p.u.* each are inserted into the system, totaling 0.02 *p.u.* After stabilization, the remaining five loads totaling 0.025 *p.u.* are added to the system, and then the electromechanical loads at the same intervals are removed.

The third test performs the integral indices (such as Integral Square Error (*ISE*) expressed in (17), Integral Absolute Error (*IAE*) (18), Integral Time Square Error (*ITSE*) (19) and Integral Square Control Efforts (*ISC*) presented in (20) [17]), to evaluates the quantitative analysis of the performance given in each above test performed. The nomenclature employed for each controller related to the results shown in this section for the simulation are *SFOPID* and *SPP*, and for the practical controllers are *PFOPID*, and *PPP* for the fractional order controller and classical pole placement, respectively. For the speed reference signal, the nomenclature adopted is *Ref* .

$$ISE = \int_0^\infty e(t)^2 dt \tag{17}$$

$$IAE = \int_0^\infty |e(t)| dt \tag{18}$$

$$ITSE = \int_0^\infty te(t)^2 dt \tag{19}$$

$$ISC = \int_0^\infty u(t)^2 dt \tag{20}$$

B. TEST 1 - TEST OF SETPOINT SPEED VARIATION

This section depicts and discusses the test of speed setpoint variation as previously described. Fig. 5 shows the results of the speed setpoint variations of the system.

The *PFOPID* presented in Fig. 5(a) has a settling time of 43.40 *s*, close to the *PPP* methodology. The simulation results depicted the same behavior presented by the practical tests; the dynamic behavior is intimate despite having fewer oscillations and a soft undershoot. Furthermore, the *PFOPID* gives less sensitivity to variation during the settling period than the other approach.

In Fig. 5(b), the *FOPID* controller response is slightly faster than the PP methodology, which presents a settling time of approximately 27.54 *s*. Also, the *PFOPID* gives a minor undershooting compared to the *PPP* methodology, which ratifies the proposed methodology and outperforms the classical approaches.

In Figs. 5(c) and 5(d) that shows a speed setpoint variation of $+0.05$ *p.u.* and $+0.1$ *p.u.*, respectively. The practical tests present a greater undershoot in both methodologies (*PFOPID* and *PPP*). Still, the worst response is presented by the *PPP* methodology, which also depicts a higher settling time as well as an elevated level of undershoot in comparison with the *PFOPID*; the simulation shows a smooth undershoot. However, it presents the same response denoted by the practical results. Fig. 6 depicts all control efforts caused by the speed setpoint variation.

Fig. 6 presents all control efforts during the speed setpoint variations. Then, it is verified that all methodologies can correct the setpoint variations performed. In addition, all methodology does not present saturation in computed control effort, and the *FOPID* methodology offers less variation than the classical pole placement methodology.

C. TEST 2 - TEST OF LOAD INSERTION

In this section, the results of the load insertion test are depicted and discussed. This test is developed as previously

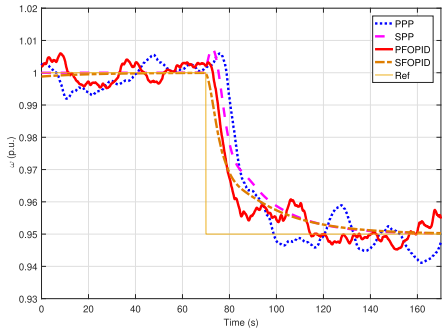

(a) $\Delta\omega_{ref} = -0.05$ p.u.

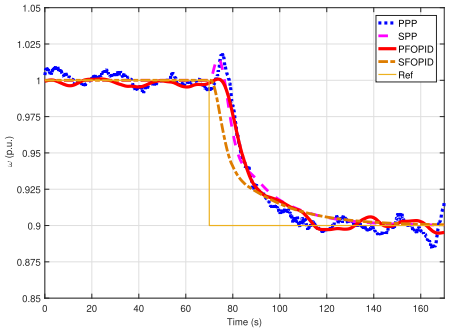

(b) $\Delta\omega_{ref} = -0.1$ p.u.

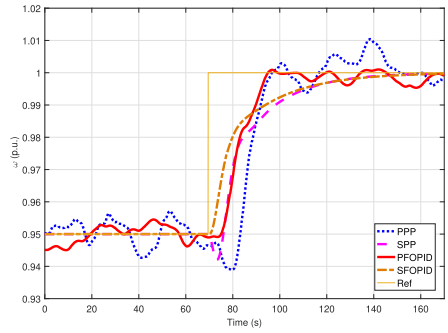

(c) $\Delta\omega_{ref} = 0.05$ p.u.

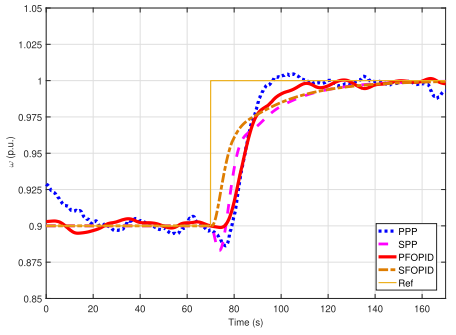

(d) $\Delta\omega_{ref} = 0.1$ p.u.

FIGURE 5. Speed setpoint variation in the system.

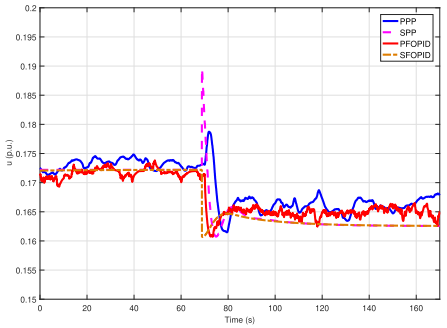

(a) $\Delta\omega_{ref} = -0.05p.u$

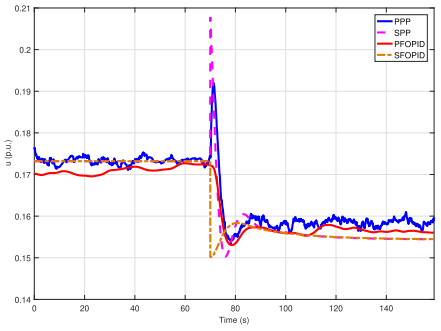

(b) $\Delta\omega_{ref} = -0.1p.u$

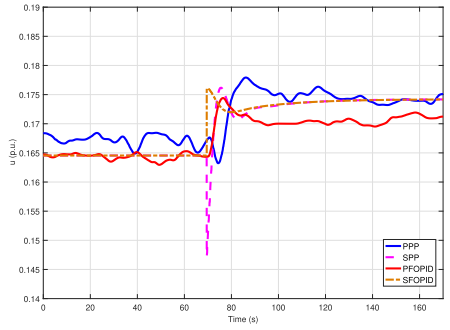

(c) $\Delta\omega_{ref} = 0.05p.u$

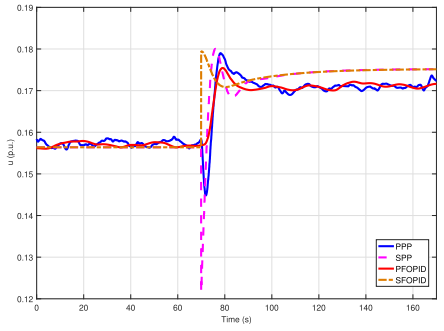

(d) $\Delta\omega_{ref} = 0.1p.u$

FIGURE 6. Control effort when occur a speed setpoint variation.

described. Fig. 7 shows the speed output oscillations of the system during the insertion or withdrawal of the mechanical load.

In Fig. 7(a), the speed deviation caused by the load insertion of 0.02 $p.u.$ is observed. Note that all methodologies corrected the deviation, but the *FOPID* methodology outperforms the classical approach. In this sense, the proposed approach presented a minor level of speed oscillation and fixed more quickly than the *PP* methodology, even in simulation and practical experiments. The same behavior is observed in Fig. 7(b). However, it presents a more

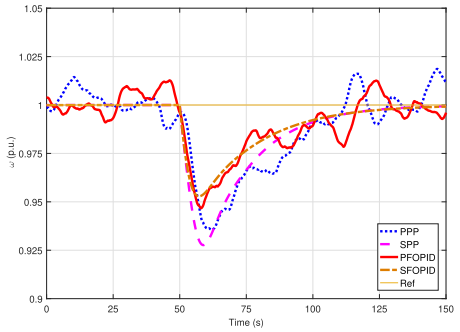

(a) $\Delta T_{load} = 0.02p.u$

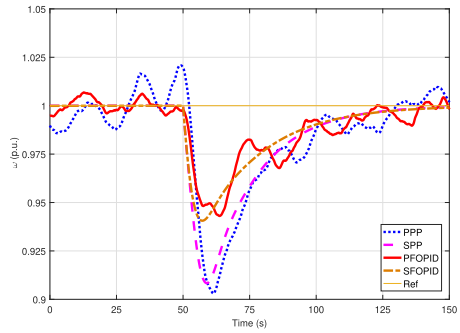

(b) $\Delta T_{load} = 0.025p.u$

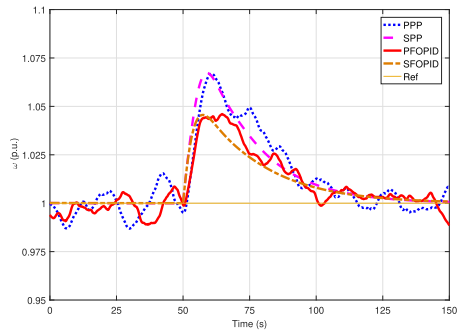

(c) $\Delta T_{load} = -0.02p.u$

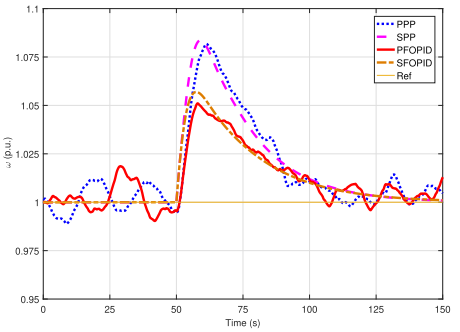

(d) $\Delta T_{load} = -0.025p.u$

FIGURE 7. Speed output when occurring a mechanical load insertion into the system.

significant difference between the *FOPID* and *PP*, where the *FOPID* denotes the improvement caused compared to the *PP* methodology.

In Figs. 7(c) and 7(d), it is possible to note that the mechanical load is withdrawn, then causes a speed oscillation in the inverted way of the previous test. These figures show that the *FOPID* methodology was able to mitigate the oscillation quickly in comparison with the *PP* methodology, and also, with the insertion of *FOPID*, the system presented a minor level of oscillation, which is the same behavior shown by the previous test. Therefore, the *FOPID* methodology gave better performance and robustness than the classical approach. In addition, the *FOPID* methodology compensates oscillations caused by load disturbance easier than the PP methodology in both cases of load insertion and withdrawal, even in simulation and experimental tests. Fig. 8 depicts all control efforts performed by the load insertion and withdrawal.

In Fig. 8, it is possible to note that all control efforts were able to correct the disturbance caused by the load insertion or withdrawal in both methodologies. Also, none of the methodologies presented saturation or prominent oscillations, so the control efforts in both methodologies are close. The practical results show the same behavior computed by simulation tests.

D. TEST 3 - ANALYSIS OF THE INTEGRAL INDICES

In this section, the integral indices are computed to perform a quantitative analysis of the control methodologies. Fig. 9 shows these computed indices related to the speed setpoint variation test.

In Fig. 9, it is worth noting that in all points of the speed variation, the indices *ISE*, *ITSE*, and *IAE*, the *FOPID* methodology presented the minor value for both simulation and practical tests.

Fig. 9(b) presents the *ISC* index. Notice that the *FOPID* methodology gives a minor control effort compared to the other approach. In this sense, the *FOPID* methodology guarantees the stability and performance of the system and also computes the minor level of control effort to correct all speed setpoint variations. In this sense, the classical *PP* presents the worst results that depict an expected performance degradation, mainly when the system gets away from the operational point. Fig. 10 shows the integral indices when the system is subject to a disturbance insertion of the mechanical load.

In Fig. 10, for all disturbance values of load insertion, the FOPID methodology presents in all evaluated indices the better performance in comparison with the *PP* methodology. These results ratify that the *FOPID* methodology is robust and improves the performance of the system, as well as is an easy way to correct load disturbance caused by insertion or withdrawal of the mechanical load, ensuring the stability and good functioning of the system. In addition, Fig. 10(b), which presents the *ISC* index, shows that all methodologies give the same energy of the control effort demanded to correct the disturbance caused by the mechanical load variations. Therefore, the proposed methodology spends the same control effort energy and performs better than the *PP* methodology, ensuring the system's stability.

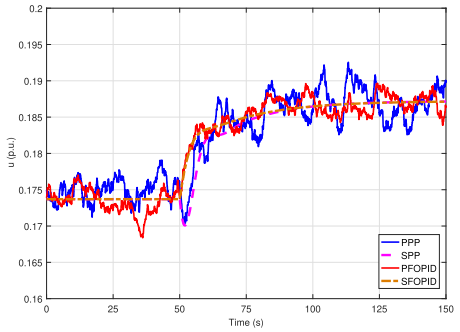

(a) $\Delta T_{load} = 0.02p.u$

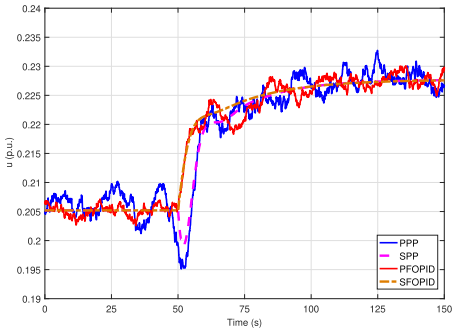

(b) $\Delta T_{load} = 0.025p.u$

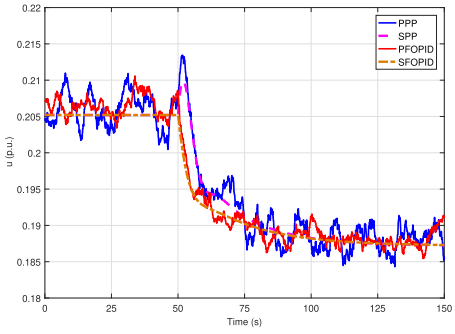

(c) $\Delta T_{load} = -0.02p.u$

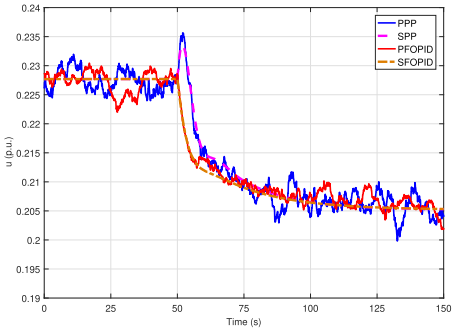

(d) $\Delta T_{load} = -0.025p.u$

FIGURE 8. Control effort when occurring a mechanical load insertion into the system.

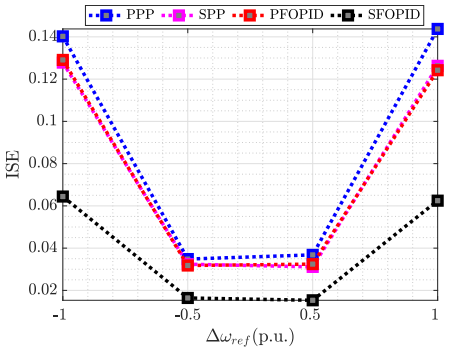

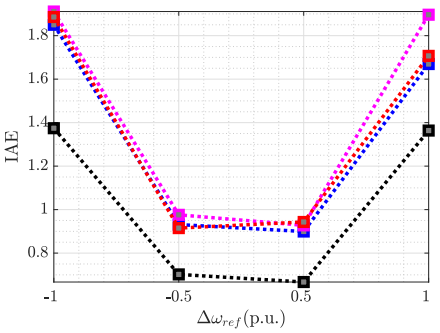

(a) *ISE* and *IAE*

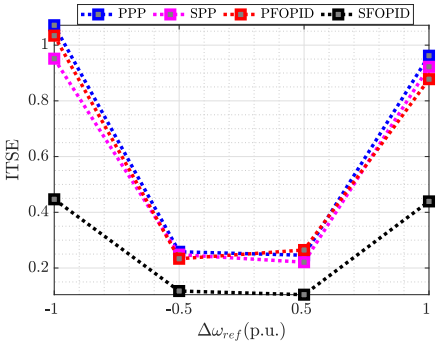

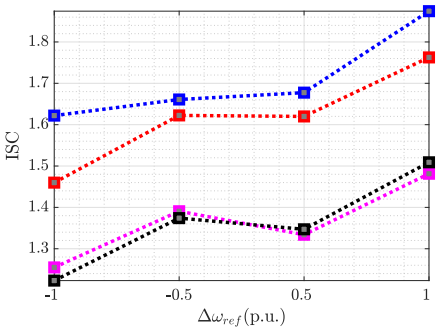

(b) *ITSE* and *ISC*

FIGURE 9. Integral indices computed taking into account the test 1 results.

E. NYQUIST STABILITY

The gain and phase margins of the system with the insertion of controllers designed using Pole Placement and Fractional-Order PID techniques are presented in the Nyquist diagram shown in Figure 11.

The phase margin of the system with the Pole Placement controller is 45.9° at the gain crossover frequency of $0.079 rad/s$, and for the system with FOPID, the phase margin is 65.5° at the gain crossover frequency of $0.121\ rad/s$. The gain margin is 7.25 dB at ω_{pc} of 0.079 rad/s for the system

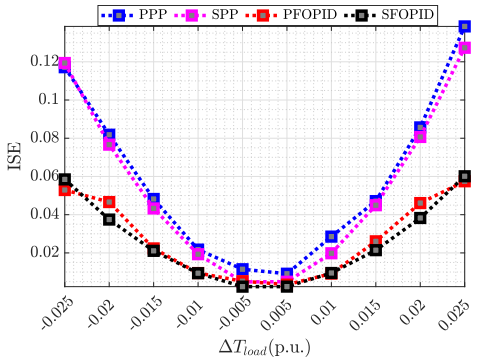

(a) *ISE* and *IAE*

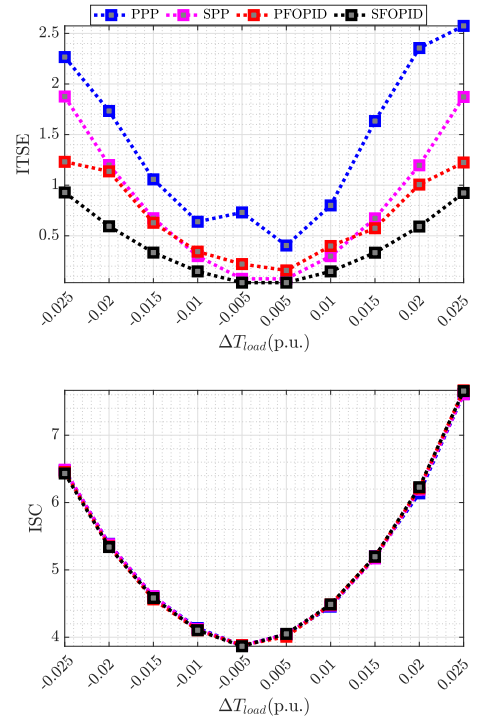

(b) *ITSE* and *ISC*

FIGURE 10. **Integral indices computed taking into account the test 2 results.**

controlled by PP and 11.9 dB at ω_{pc} of 0.433 rad/s with the FOPID controller.

The analysis of the Nyquist diagram indicates that both controlled systems are stable, given that the geometric place crosses the negative real axis at values smaller than $-1+j0$,

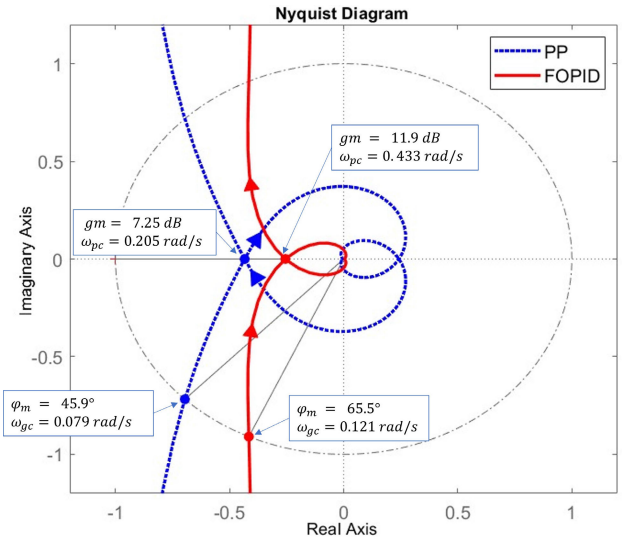

FIGURE 11. **Direct loop Nyquist curve with the insertion of controllers.**

with a positive phase margin and gain margin. Additionally, it is observed that the geometric locus of the system with the pole placement controller is closer to the point $-1+j0$, causing its step response to have a higher overshoot and a longer settling time.

Finally, the inclusion of all controllers demonstrates a degree of robustness. This is because, to achieve satisfactory performance, the phase margin should be above 30°, and the gain margin should be greater than 6 dB [37].

F. QUALITATIVE ANALYSIS

The comparative analysis between studies applied to hydraulic turbines and using Fractional Order Proportional-Integral-Derivative (FOPID) controllers reveals a predominance of simulated approaches, as detailed in Table 4. Most of these studies employ optimization methods to determine controller parameters, with Genetic Algorithms (GA) and Particle Swarm Optimization (PSO) being the most prominent. In applying fractional-order controllers in simulated systems, the Oustaloup approximation method is widely used to estimate an integer order transfer function.

The performance evaluation of developed controllers highlights that systems with fractional controllers or incorporating optimization methods show superior settling time and overshoot results compared to systems adopting classical controllers. Few studies explore the control effort required to achieve the desired performance.

Facing this scenario, the present work aims to fill this gap by comprehensively analyzing PID and FOPID controller applications. This study seeks not only to compare existing approaches but also to provide valuable insights into the control effort required to optimize the performance of the studied systems.

V. CONCLUSION

This paper has presented the simulation and experimental evaluation of the design and application of the

TABLE 4. Qualitative analysis.

Attribute Category	Goals	Ref.
Controlled Process	Stability analysis of the hydraulic turbine fractional-order interval parameter time-delay system. The system is of non-minimum order.	[25]
	Frequency control of a dual area hybrid microgrid (DHM) that comprises solar thermal systems alongside biodiesel-powered generators.	[11]
	Control of speed governor of hydraulic turbines in hydroelectric plants.	[27]
	Speed control of a non-linear model of hydraulic turbines, also subject to a load disturbance.	[26]
	Control system for the position of a regulator in a nonlinear, non-minimum phase hydro turbine of a 250 MW hydropower generation unit.	[38]
	Speed control of an Electric Vehicle (EV).	[39]
	Winding system used in the industry to achieve constant voltage control by regulating the motor torque.	[40]
Types of Controllers	PID, PID plus second order derivative (PID2D), FOPID and FOPID plus second order derivative (FOPID2D).	[25]
	Cascaded PI-TID (Proportional Integral Tilt-Integral-Derivative), PID and TID controller.	[11]
	PID and FOPID controller.	[27]
	PID and FOPID controller.	[26]
	Complimentary Sliding-Mode Controller (CSMC) and PID controller.	[38]
	Fuzzy FOPID, fuzzy integer-order PID (IOPID), FOPID, and traditional IOPID controllers.	[39]
	PID and FOPID controller.	[40]
Optimization Method	Uses the edge theorem and the D-decomposition method to perform the computing of the stability region for the controller parameters.	[25]
	Uses the chaotic butterfly optimization (CBOA) technique to attain the tuned gain constraints of the cascaded PI-TID controller.	[11]
	The Non-dominated Sorting Genetic Algorithm II (NSGAII) is employed in conjunction with the Iterative Chaotic Map with Infinite Collapses (ICMIC) method to optimize the parameters of the FOPID controller. The ISE and the ITSE constitute the objective functions.	[27]
	It uses the Particle Swarm Optimization (PSO) algorithm to find the optimal parameters for the controller and the objective function based on the ITAE criterion.	[26]
	Does not present any optimization method.	[38]
	Key elements in the Takagi-Sugeno fuzzy inference system are optimized through the Ant Colony Optimization (ACO) algorithm. The performance of the optimized controller is then compared with Fuzzy FOPID controllers utilizing Genetic Algorithms (GA) and Particle Swarm Optimization (PSO) algorithms.	[39]
	The optimization method is implemented using the Genetic Algorithm (GA) combined with FMINCON (non-linear optimization) to determine the five adjustable parameters of the FOPID controller.	[40]
Approximation Method	Uses the piecewise linear model as an approximation to the nonlinear system.	[25]
	It does not employ any approximation methods.	[11]
	The Oustaloup approximation method implements fractional-order transfer functions in simulations.	[27]
	Utilizes a modified Oustaloup approximation filter, which is more accurate than others.	[26]
	It does not employ any approximation methods.	[38]
	The fractional-order operator is approximated to an integer-order rational function using the Oustaloup approximation method.	[39]
	It does not employ any approximation methods.	[40]
Performance Evaluation	Presents a simulated study in which the system with the FOPID2D controller demonstrated superior robust stability.	[25]
	It concerns a simulated project in which the PI-TID controller in cascade configuration ensures the system's robustness, leading to disturbance rejection.	[11]
	Presents a simulated study where the results obtained by the system with a FOPID controller ensure stability and robustness to variations in system parameters under load conditions.	[27]
	It is a simulation of a 10% load disturbance using the Simulink software in MATLAB. The results reveal that the system with the FOPID controller outperforms the PID system, showing lower overshoot and settling time. Both systems demonstrated effectiveness in disturbance rejection.	[26]
	In this study, simulations are conducted using the MatLab Simulink environment for a 250 MW Hydroelectric Turbine Control System (HTCS) model.The results demonstrate the effectiveness of the CSMC throughout the startup process, subsynchronous, and supersynchronous operating modes.Considering the results obtained through the reduced-scale laboratory model, it is observed that both the settling time and overshoot for all prototype performance parameters considered in this study are reduced when the hydro-turbine is controlled by CSMC compared to PID control. Thus, the developed controller exhibits a notable error-tracking capability, providing a more agile response to transient states.	[38]
	Presents a simulated study where the results obtained by the system with Fuzzy FOPID controller based on ACO ensure effectiveness, stability, and robustness when employed in electric vehicle speed tracking. It achieves a shorter settling time and lower overshoot than the other analyzed controllers.	[39]
	The simulated study reveals that the FOPID controller outperforms the classical PID in various aspects, such as rise time, steady-state, peak, and overshoot in the analysis of the step response of the closed-loop system. This superiority extends to gain robustness, load variation, high-frequency noise, and output interference. In summary, with a simple implementation process, FOPID demonstrates better control characteristics, robustness, tracking accuracy, and temporal response.	[40]
Control Signal	This information is not addressed in the study.	[25]
	This information is not addressed in the study.	[11]
	Although some results regarding the control signal output show high-amplitude oscillations, no saturation occurs.	[27]
	This information is not addressed in the study.	[26]
	This information is not addressed in the study.	[38]
	The Fuzzy FOPID controller stands out by minimizing control effort compared to the Fuzzy IOPID controller, demonstrating superior performance due to the high amplitude values associated with conventional IOPID and FOPID. Thus, the primary advantage of the FOPID fuzzy controller lies in its ability to reduce control effort.	[39]
	This information is not addressed in the study.	[40]

fractional-order controller in emulation of hydraulic turbines in a small-scale developed testbed system, with that aimed to reduce the problems related to the speed regulation of the existing hydraulic turbines in power generation systems of hydroelectric plants.

For this, two controllers have been investigated, one of integer order and one of fractional order, and both controllers were applied to the system in a computational environment and in a non-linear system that represents a small-scale power generation system. The controllers' implementation was performed through a development platform that uses *Arduíno Due* controller to insert the speed governor into this testbed system.

Analyzing the responses of the practical tests carried out in a non-minimum phase system, it was found that in all tests, the system with the fractional order speed regulator presented a smaller overshoot and undershoot as well as a minor level of speed oscillations. However, the settling time of both controllers was similar in some cases.

Observing the performance index values obtained through varying setpoint speed, it is discernible that the integral square error (ISE) exhibited less variation in practical tests with the fractional-order PID controller. Upon varying the reference speed signal from 0.9 p.u. to 1.0 p.u., 0.1242 was obtained with the FOPID controller and 0.1438 with the conventional controller, representing an improvement of approximately 16%. However, upon analysis of the performance index for the integral absolute error (IAE), it is evident that the pole-placement controller improved over the fractional controller, albeit by a maximum of 4%. Upon scrutinizing the performance index of the integral square control signal (ISC), it is observed that the speed regulator with the fractional PID exhibited the lowest control effort, up to 10%.

After careful analysis of the practical outcomes observed during the insertion and removal of load, it is evident that the system equipped with the FOPID controller demonstrated significantly superior performance compared to the classical controller. Specifically, upon inserting 0.025 p.u. of load into the generation system, the performance index of the FOPID controller was recorded at 0.0575. In contrast, that of the Pole Placement controller was noted at 0.1345, indicating a performance that was approximately 140% higher than that of the fractional controller. Moreover, when considering the other indices, IAE and ITSE, the practical implementation of the FOPID controller exhibited a performance that was 180% superior compared to the classical controller. It is noteworthy, however, that the control effort developed by both controllers was comparable.

Although the classic controller has been tuning techniques easier, the responses have more sensibility to the undesirable dynamical system effects, as high transient signal values can cause loss of energy generation or damage to equipment. Therefore, evaluating the results, the speed regulation control loop of the hydraulic turbine presented a dynamic performance improvement when the FOPID controller was applied to the speed governor presented in this work. Thus making the energy generation system more efficient and safer for the system studied in this paper.

While executing this project, we encountered various challenges, with one prominent difficulty being the necessity to construct a small-scale generation system and replicate the dynamic behavior of the hydraulic turbine to facilitate practical tests involving speed setpoint variation and load insertion and removal. As a result, our further work and subsequent endeavors will focus on developing and implementing other speed regulation controllers. These may include the fractional-order PID controller tuned utilizing pole placement methodologies and controllers that employ optimization algorithms.

APPENDIX A
VALUES

TABLE 5. Values of design parameters.

Parameters		Unit	Value
Settling time	t_s	s	45
Maximum overshoot	M_{ss}	-	0.1
Error	e	%	5
Damping factor	ζ	-	0.5912
Natural frequency	ω_n	rad/s	0.1126
Low frequency	ω_l	rad/s	0.0398
High frequency	ω_h	rad/s	0.3185
Sample time	T	s	1
Gain margin	gm	dB	6
Phase margin	φ_m	°	65
Gain crossover frequency	ω_{gc}	rad/s	0.1126
Phase crossing frequency	ω_{pc}	rad/s	0.5631

ACKNOWLEDGMENT

This research, carried out within the scope of the Samsung-UFAM Project for Education and Research (SUPER), according to Article 39 of Decree n°10.521/2020, was funded by Samsung Electronics of Amazonia Ltda., under the terms of Federal Law n°8.387/1991 through agreement 001/2020, signed with Federal University of Amazonas (UFAM) and Federal Institute of Amazonas (IFAM) Teaching, Research, Extension and Internalization Support Foundation (FAEPI), Brazil. The authors thank the scholarship and financial support in part from the Amazonas State Research Support Foundation (FAPEAM), Foundation Coordination for the Improvement of Higher Education Personnel (CAPES), National Council for Scientific and Technological Development (CNPq) and UFAM. Thanks to the College of Technology of UFAM (FT/UFAM) Control Systems (LC) and Electrical Machines Laboratory (LME) at UFAM and the e-Controls Research Group.

REFERENCES

[1] H. Fang, X. Yuan, and P. Liu, "Active–disturbance–rejection–control and fractional–order–proportional–integral–derivative hybrid control for hydroturbine speed governor system," *Meas. Control*, vol. 51, nos. 5–6, pp. 192–201, Jun. 2018.

[2] P. Kundur, *Power Systems Stability and Control*, vol. 1. New York, NY, USA: McGraw-Hill, 1994.
[3] S. J. Chapman, *Electric Machinery Fundamentals*, 5th ed. New York, NY, USA: McGraw-Hill, 2012.
[4] P. W. Sauer, *Power System Dynamics and Stability: With Synchrophasor Measurement and Power System Toolbox*, 2nd ed. Hoboken, NJ, USA: Wiley, 2018.
[5] D. Borkowski, "Analytical model of small hydropower plant working at variable speed," *IEEE Trans. Energy Convers.*, vol. 33, no. 4, pp. 1886–1894, Dec. 2018.
[6] P. K. Ray, S. R. Paital, A. Mohanty, Y. S. E. Foo, A. Krishnan, H. B. Gooi, and G. A. J. Amaratunga, "A hybrid firefly-swarm optimized fractional order interval type-2 fuzzy PID-PSS for transient stability improvement," *IEEE Trans. Ind. Appl.*, vol. 55, no. 6, pp. 6486–6498, Nov. 2019.
[7] W. Group Prime Mover and E. Supply, "Hydraulic turbine and turbine control models for system dynamic studies," *IEEE Trans. Power Syst.*, vol. 7, no. 1, pp. 167–179, Feb. 1992.
[8] M. Beus, H. Pandžic, and R. Sirovina, "Hydro power unit speed control based on an MPC algorithm," in *Proc. 7th Int. Conf. Smart Sustain. Technol. (SpliTech)*, Jul. 2022, pp. 1–6.
[9] T. L. Filbert and L. Wozniak, "Speed loop cancellation governor for hydrogenerators. II. Application," *IEEE Trans. Energy Convers.*, vol. 3, no. 1, pp. 91–94, Mar. 1988.
[10] L. Wozniak and T. L. Filbert, "Speed loop cancellation governor for hydrogenerators. I. Development," *IEEE Trans. Energy Convers.*, vol. 3, no. 1, pp. 85–90, Mar. 1988.
[11] M. Bhuyan, D. C. Das, A. K. Barik, and S. C. Sahoo, "Performance assessment of novel solar thermal-based dual hybrid microgrid system using CBOA optimized cascaded PI-TID controller," *IETE J. Res.*, vol. 2022, pp. 1–18, Jun. 2022.
[12] I. Kamwa, D. Lefebvre, and L. Loud, "Small signal analysis of hydro-turbine governors in large interconnected power plants," in *Proc. IEEE Power Eng. Soc. Winter Meeting Conf.*, vol. 2, New York, NY, USA, 2002, pp. 1178–1183.
[13] C. K. Shiva and V. Mukherjee, "Comparative performance assessment of a novel quasi-oppositional harmony search algorithm and internal model control method for automatic generation control of power systems," *IET Gener., Transmiss. Distrib.*, vol. 9, no. 11, pp. 1137–1150, Aug. 2015.
[14] M.-H. Khooban, M. Gheisarnejad, N. Vafamand, M. Jafari, S. Mobayen, T. Dragicevic, and J. Boudjadar, "Robust frequency regulation in mobile microgrids: HIL implementation," *IEEE Syst. J.*, vol. 13, no. 4, pp. 4281–4291, Dec. 2019.
[15] M. Fakhari Moghaddam Arani and Y. A. I. Mohamed, "Cooperative control of wind power generator and electric vehicles for microgrid primary frequency regulation," *IEEE Trans. Smart Grid*, vol. 9, no. 6, pp. 5677–5686, Nov. 2018.
[16] H. Li, Y. Luo, and Y. Chen, "A fractional order proportional and derivative (FOPD) motion controller: Tuning rule and experiments," *IEEE Trans. Control Syst. Technol.*, vol. 18, no. 2, pp. 516–520, Mar. 2010.
[17] F. A. D. C. Ayres, I. Bessa, V. M. B. Pereira, N. J. da Silva Farias, A. R. de Menezes, R. L. P. de Medeiros, J. E. Chaves, M. K. Lenzi, and C. T. da Costa, "Fractional order pole placement for a buck converter based on commensurable transfer function," *ISA Trans.*, vol. 107, pp. 370–384, Dec. 2020. [Online]. Available: https://www.sciencedirect.com/science/article/pii/S0019057820303153
[18] P. Lino, G. Maione, R. Garrappa, and S. Holm, "An approach to optimal integer and fractional-order modeling of electro-injectors in compression-ignition engines," *Control Eng. Pract.*, vol. 115, Oct. 2021, Art. no. 104890. [Online]. Available: https://www.sciencedirect.com/science/article/pii/S0967066121001672
[19] J. Lai, X. Yin, X. Yin, and L. Jiang, "Fractional order harmonic disturbance observer control for three-phase LCL-type inverter," *Control Eng. Pract.*, vol. 107, Feb. 2021, Art. no. 104697.
[20] D. Pullaguram, S. Mishra, N. Senroy, and M. Mukherjee, "Design and tuning of robust fractional order controller for autonomous microgrid VSC system," *IEEE Trans. Ind. Appl.*, vol. 54, no. 1, pp. 91–101, Jan. 2018.
[21] I. Pan, S. Das, and A. Gupta, "Handling packet dropouts and random delays for unstable delayed processes in NCS by optimal tuning of controllers with evolutionary algorithms," *ISA Trans.*, vol. 50, no. 4, pp. 557–572, Oct. 2011. [Online]. Available: https://www.sciencedirect.com/science/article/pii/S0019057811000498
[22] S. Das, I. Pan, and S. Das, "Fractional order fuzzy control of nuclear reactor power with thermal-hydraulic effects in the presence of random network induced delay and sensor noise having long range dependence," *Energy Convers. Manage.*, vol. 68, pp. 200–218, Apr. 2013. [Online]. Available: https://www.sciencedirect.com/science/article/pii/S0196890413000228
[23] K. Singh, "Load frequency regulation by de-loaded tidal turbine power plant units using fractional fuzzy based PID droop controller," *Appl. Soft Comput.*, vol. 92, Jul. 2020, Art. no. 106338. [Online]. Available: https://www.sciencedirect.com/science/article/pii/S1568494620302787
[24] I. Pan and S. Das, "Fractional order AGC for distributed energy resources using robust optimization," *IEEE Trans. Smart Grid*, vol. 7, no. 5, pp. 2175–2186, Sep. 2016.
[25] T. Tian, J. Lv, and J. Tang, "Stability comparison of different controllers for hydraulic turbine fractional order interval parameter time-delay system," *Syst. Sci. Control Eng.*, vol. 11, no. 1, pp. 1–15, Dec. 2023.
[26] X. Yuan, "Fractional order control for hydraulic turbine system based on nonlinear model," in *Foundations and Applications of Intelligent Systems*, 2014, pp. 287–296.
[27] Z. Chen, X. Yuan, B. Ji, P. Wang, and H. Tian, "Design of a fractional order PID controller for hydraulic turbine regulating system using chaotic non-dominated sorting genetic algorithm II," *Energy Convers. Manage.*, vol. 84, pp. 390–404, Aug. 2014.
[28] F. A. Junior, C. C. Junior, R. Medeiros, W. B. Junior, C. Neves, M. Lenzi, and G. Veroneze, "A fractional order power system stabilizer applied on a small-scale generation system," *Energies*, vol. 11, no. 8, p. 2052, Aug. 2018. [Online]. Available: https://www.mdpi.com/1996-1073/11/8/2052
[29] K. J. Åström and T. Hägglund, *PID Controllers: Theory, Design, and Tuning*, 2nd ed. NC, USA: International Society for Measurement and Control, 1995.
[30] R. Vilanova and A. Visioli, *Fractional-Order PID: In Advances in Industrial Control—PID Control in the Third Millennium, Lessons Learned and New Approaches*. London, U.K.: Springer, 2012.
[31] B. Strah, O. Kuljaca, and Z. Vukic, "Speed and active power control of hydro turbine unit," *IEEE Trans. Energy Convers.*, vol. 20, no. 2, pp. 424–434, Jun. 2005.
[32] D. Xue, C. Zhao, and Y. Chen, "Fractional order PID control of a DC-motor with elastic shaft: A case study," in *Proc. Amer. Control Conf.*, Minneapolis, MN, USA, 2006.
[33] M. R. Faieghi and A. Nemati, *On Fractional-Order PID Design in Applications of MATLAB: In Science and Engineering*. London, U.K.: IntechOpen, 2011.
[34] D. Puangdownreong, "Fractional order PID controller design for DC motor speed control system via flower pollination algorithm," *ECTI Trans. Electr. Eng., Electron., Commun.*, vol. 17, no. 1, pp. 14–23, Sep. 2019.
[35] D. Valério and J. S. Costa, *An Introduction to Fractional Control*, vol. 91. London, U.K.: IET Control Engineering Series, 2013.
[36] I. D. Landau and G. Zito, *Digital Control Systems: Design, Identification and Implementation* (Communications and Control Engineering). Cham, Switzerland: Springer, 2006.
[37] K. Ogata, *Modern Control Engineering*, 2nd ed. Upper Saddle River, NJ, USA: Prentice-Hall, 2009.
[38] R. Kumari, K. K. Prabhakaran, K. Desingu, T. R. Chelliah, and S. V. A. Sarma, "Improved hydroturbine control and future prospects of variable speed hydropower plant," *IEEE Trans. Ind. Appl.*, vol. 57, no. 1, pp. 941–952, Jan. 2021.
[39] M. A. George, D. V. Kamat, and C. P. Kurian, "Electronically tunable ACO based fuzzy FOPID controller for effective speed control of electric vehicle," *IEEE Access*, vol. 9, pp. 73392–73412, 2021.
[40] F. Meng, S. Liu, and K. Liu, "Design of an optimal fractional order PID for constant tension control system," *IEEE Access*, vol. 8, pp. 58933–58939, 2020.

CLAUDIA SABRINA MONTEIRO DA SILVA received the Graduate and master's degrees in electrical engineering from the Federal University of Amazonas—UFAM, in 2019 and 2022, respectively, where she is currently pursuing the Ph.D. degree with the Graduate Program in Electrical Engineering (PPGEE). Her main research interests include control and dynamics of power systems using frequency response and fractional order techniques.

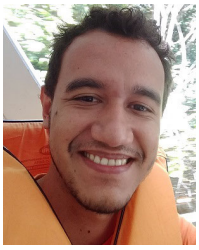

NEI JUNIOR FARIAS DA SILVA received the Graduate and master's degrees in electrical engineering—electrotechnical from the Federal University of Amazonas—UFAM, in 2018 and 2021, respectively, where he is currently pursuing the Ph.D. degree with the Graduate Program in Electrical Engineering. During the undergraduate and master's degrees, he was a Monitor of the Disciplines of Electrical Circuits and General Electricity Laboratory and participated in four extension projects and a research and development project as a Newton Fund Fellow in partnership with Coventry University. He was an Intern with Engecrim Engenharia, where he participated in and followed projects for electrical installations. His research interests include emulating electrical power systems, controlling and stabilizing electrical power systems, and DC/DC power converters.

FLORINDO A. DE C. AYRES JÚNIOR received the B.Sc., M.Sc., and Ph.D. degrees from the Federal University of Pará, Brazil, in 2013, 2014, and 2018, respectively. He is currently a Professor and the Head of the Department of Electricity (DE) and a Coordinator of the Control Systems Laboratory (LSC), Federal University of Amazonas (UFAM), Brazil, where he is also a member of the Control Systems Group named e-CONTROLS, the Electrical Engineering Post Graduation Program (PPGEE), and the Brazilian Automatic Society (SBA). His main research interests include process modeling of electrical and industrial systems, emphasizing studying and applying fractional order modeling, identification, and control systems.

RENAN LANDAU PAIVA DE MEDEIROS received the B.E., M.Sc., and Ph.D. degrees in electrical engineering from the Federal University of Pará (UFPA), Brazil, in 2013, 2014, and 2018, respectively.

He is currently an Associate Professor with the Department of Electrical Engineering, UFAM. He has experience in electrical engineering, emphasizing automation and control of industrial and electrical power systems, multivariable robust control, and application. Since 2017, he has been a full-time Researcher with the e-CONTROLS, a research group interested in any topics of dynamic and control systems, with an emphasis on electric power system control. His research interests include nonlinear control, multivariable robust control, modeling, and designing a robust control for electrical power systems.

LUIZ EDUARDO SALES E SILVA received the B.Sc. and M.Sc. degrees in electrical engineering from the Federal University of Amazonas (UFAM), Brazil, in 2011 and 2014, respectively. He is currently pursuing the Ph.D. degree with the Federal University of Pará (UFPA), Brazil. Since 2015, he has been an Assistant Professor with the Department of Electricity, UFAM. His research interests include electrical power systems, emphasizing smart grids, distributed energy resources, electric vehicles and modeling, control, and monitoring of low voltage distribution networks.

VICENTE FERREIRA DE LUCENA JR. (Senior Member, IEEE) was born in São Paulo, Brazil, in 1965. He received the B.Sc. degree in electrical engineering from the Federal University of Amazonas, in 1987, the M.S. degree in electrical engineering from the Federal University of Paraiba (currently Federal University of Campina Grande), in 1993, and the Ph.D. degree in electrical engineering (emphasis in industrial automation and software engineering) from Universität Stuttgart, Germany, in 2002. After several years of industry experience in Manaus, he joined the Academic Career with UFAM and IFAM. Since 1991, he has been a Lecturer/Professor with the Federal University of Amazonas. Since 2019, he has been a Full Professor. He teaches courses in electrical engineering and computer engineering programs, both of which belong to the Faculty of Technology. He is also a Permanent Professor of the Postgraduate Program in Electrical Engineering (PPGEE) and Postgraduate Program in Computer Science (PPGI), Federal University of Amazonas (Ph.D. and master's courses). He was a Career Professor with the Federal Institute of Education, Science, and Technology of Amazonas (formerly ETFAM and CEFET-AM), from 1989 to 2012. His research interests include electrical engineering and computer science, with an emphasis on embedded systems and software engineering, working recently on the following subjects: industrial automation systems, applications of cyber-physical systems, new applications for industry (industry 4.0) software reuse techniques, applications for electronic health and assistive technologies (eHealth systems), intelligent environments, and ambient intelligence (home and industrial usage). He has coordinated several research and development projects related to these topics with the financial support of CNPq, FAPEAM, FINEP, and SUFRAMA; and companies located in the Industrial Hub of Manaus. He was a Representative of the Scientific Community in the Superior Council of the Foundation for Research Support of the State of Amazonas—FAPEAM, from 2003 to 2004, and as a Teaching Representative (elected by peers) in the Research Chamber of that institution, from 2012 to 2018. He received the Title of a Senior Member of ACM, in 2013, and a Senior Member of ISA, in 2014.